Cell Metabolism
Short Article

Intestinal Specific LXR Activation Stimulates Reverse Cholesterol Transport and Protects from Atherosclerosis

Giuseppe Lo Sasso,[1] Stefania Murzilli,[1] Lorena Salvatore,[1] Ilenia D'Errico,[1] Michele Petruzzelli,[1] Paola Conca,[3] Zhao-Yan Jiang,[4,5] Laura Calabresi,[3] Paolo Parini,[4,5] and Antonio Moschetta[1,2,*]
[1]Laboratory of Lipid Metabolism and Cancer, Department of Translational Pharmacology, Consorzio Mario Negri Sud, 66030 Santa Maria Imbaro, Chieti, Italy
[2]Clinica Medica "A. Murri," Department of Internal and Public Medicine, University of Bari, 70124 Bari, Italy
[3]Center E. Grossi Paoletti, Department of Pharmacological Sciences, Università degli Studi di Milano, 20133 Milano, Italy
[4]Division of Clinical Chemistry, Department of Laboratory Medicine
[5]Molecular Nutrition, Department of Biosciences and Nutrition
Karolinska Institutet at Huddinge University Hospital, S-141 86 Stockholm, Sweden
*Correspondence: moschetta@negrisud.it
DOI 10.1016/j.cmet.2010.07.002

SUMMARY

Several steps of the HDL-mediated reverse cholesterol transport (RCT) are transcriptionally regulated by the nuclear receptors LXRs in the macrophages, liver, and intestine. Systemic LXR activation via synthetic ligands induces RCT but also causes increased hepatic fatty acid synthesis and steatosis, limiting the potential therapeutic use of LXR agonists. During the last few years, the participation of the intestine in the control of RCT has appeared more evident. Here we show that while hepatic-specific LXR activation does not contribute to RCT, intestinal-specific LXR activation leads to decreased intestinal cholesterol absorption, improved lipoprotein profile, and increased RCT in vivo in the absence of hepatic steatosis. These events protect against atherosclerosis in the background of the LDLR-deficient mice. Our study fully characterizes the molecular and metabolic scenario that elects the intestine as a key player in the LXR-driven protective environment against cardiovascular disease.

INTRODUCTION

In the reverse cholesterol transport (RCT) pathway, excess cholesterol fluxed from peripheral cells to HDL is transported to the liver for subsequent elimination as bile acids and neutral steroids (Rader, 2003). While LDL, formed by the metabolism of very low-density lipoproteins (VLDLs), and chylomicron remnant particles are considered proatherosclerotic (Zilversmit, 1979), HDLs are considered antiatherogenic due to their ability to stimulate RCT (Linsel-Nitschke and Tall, 2005; Rader, 2002) and to their antioxidant and anti-inflammatory properties (Navab et al., 2000). At molecular level, one of the first steps of RCT is mediated by ATP-binding cassette (ABC) transporter A1 (ABCA1), which effluxes phospholipids and cholesterol from cell membrane to lipid-poor ApoAI to generate pre-βHDL (Oram and Vaughan, 2000). HDL further acquires cholesterol via ABCG1- and SR-BI-mediated efflux (Klucken et al., 2000; Wang et al., 2004).

Liver X receptors (LXRs) α (NR1H3) and β (NR1H2), members of the nuclear receptor transcription factor family, are critical for the control of lipid homeostasis and respond to physiological concentrations of sterols (Janowski et al., 1996; Willy and Mangelsdorf, 1997). Activation of LXR by synthetic agonists reduces the body load of cholesterol by stimulating the RCT pathway through the induction of a wide range of target genes such as ABCA1, ABCG1, ABCG5, ABCG8, and apolipoprotein E (ApoE) (Repa et al., 2000b, 2002; Venkateswaran et al., 2000; Laffitte et al., 2001). However, the potential for LXR agonists as treatment option for atherosclerosis (Joseph et al., 2002; Terasaka et al., 2003; Kratzer et al., 2009) is hampered by the activation of key genes critical for hepatic de novo lipogenesis (Repa et al., 2000a; Schultz et al., 2000). Hence, systemic LXR activation induces RCT but also causes hypertriglyceridemia and hepatic steatosis (Grefhorst et al., 2002).

Recently, the participation of intestine in the regulation of RCT has become more evident, with the crucial role of this organ for the maintenance of plasma HDL (Brunham et al., 2006a; Brunham et al., 2006b) and the direct secretion of plasma-derived cholesterol into the intestinal lumen (van der Velde et al., 2007), both processes improved by LXR activation. Hence, new strategies aimed to specifically target LXR in the intestine were proposed in order to avoid the hepatic steatosis observed after activation of LXR in the liver. In this study, we provide evidence that the constitutive activation of LXRα in the intestinal epithelium reduces atherosclerosis by decreasing intestinal cholesterol absorption, improving lipoprotein composition, and stimulating RCT without hepatic lipid accumulation.

RESULTS

Intestinal LXR Decreases Cholesterol Absorption and Induces RCT

To elucidate the role of selective intestinal LXR activation in lipid metabolism and atherosclerosis, we generated a transgenic

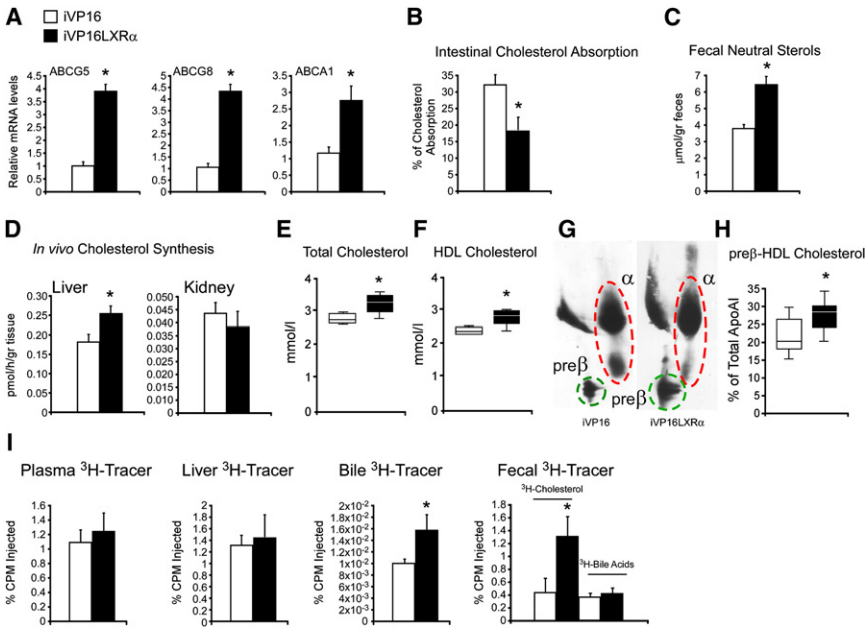

Figure 1. Characterization of iVP16LXRα Transgenic Mice

(A) Expression of LXRα target genes in the intestine of iVP16LXRα was measured by real-time quantitative PCR. ABCG5, ABCG8, and ABCA1 mRNA levels were upregulated in the intestine of iVP16LXRα. The results are shown as mean ± SEM (n = 6 for each genotype).

(B) Fractional cholesterol absorption of iVP16LXRα versus iVP16 mice. Intestinal cholesterol absorption was measured using the fecal dual-isotope method as described in the Supplemental Experimental Procedures and shows a 40% reduction in iVP16LXRα compared to control mice.

(C) Increased fecal neutral sterol excretion was measured in iVP16LXRα compared to iVP16 mice as described in the Supplemental Experimental Procedures.

(D) The rates of in vivo cholesterol synthesis in the liver and kidney (extrahepatic control tissue) were measured 60 min after intraperitoneal injection of ^{3}H-water precursor. Reduced cholesterol absorption determines a compensatory increase in liver cholesterol biosynthesis. The results are shown as mean ± SEM (n = 6 for each genotype).

(E) Box and whisker plots of plasma total cholesterol measurements with the bottom and the top of the boxes representing the 25th and 75th percentile, i.e., lower and upper quartile, respectively, and the band near the middle of the box representing the 50th percentile, i.e., median, and the ends of the whiskers the minimum and the maximum of all the data for a total of n = 12 mice.

(F) Box and whisker plots of cholesterol HDL measurements of n = 12 mice.

(G) HDL subclasses in iVP16LXRα and iVP16. HDL subclasses were separated by two-dimensional gel electrophoresis in pre-β and α migrating particles and transferred onto a nitrocellulose membrane, which were detected with an anti-apolipoprotein A-I antibody.

(H) Box and whisker plots of pre-βHDL fractions as percent of total Apo A-I. of n = 12 mice.

(I) Intestinal-specific LXR activation impact on macrophage-specific cholesterol transport (RCT) in vivo. Macrophage-derived ^{3}H-cholesterol content (from left to right) in plasma, liver, bile, and feces was measured by liquid scintillation counting. Data analysis shows that intestinal-specific LXR activation is able to induce macrophage-mediated RCT resulting in augmented fecal cholesterol removal. The results are shown as mean ± SEM (n = 6 for each genotype) and are expressed as percent of radioactivity injected. *p < 0.05 iVP16LXRα versus VP16.

mouse model in which the constitutively activated form of LXRα (VP16LXRα) was under the control of the enterocyte-specific *Villin* promoter (Madison et al., 2002). As controls, transgenic mice specifically expressing in the intestine VP16 (iVP16) were generated. iVP16LXRα mice were fertile and were born at the expected Mendelian frequencies. iVP16LXRα mice expressed the VP16LXRα in the entire length of the intestine (see Figures S1A and S1B available online). To confirm the functionality of the VP16LXRα transgene expression, we measured the mRNA and protein expression of known LXR target genes in the intestine. As shown in Figure 1A, ABCG5, ABCG8, and ABCA1 mRNA levels (Figure 1A), as well as ABCA1 protein (Figures S1B and S1D), were upregulated in the intestine of iVP16LXRα. Tissue-specific activation of the LXR-mediated transcriptional machinery was confirmed by the absence of modulation of LXR target genes ABCG5 and ABCG8 in the liver of transgenic mice (Figure S1E).

The induction of ABCG5 and ABGC8 in iVP16LXRα mice was accompanied by a 40% reduction in cholesterol absorption compared to control iVP16 mice (Figure 1B). The reduction in cholesterol absorption was coupled with an increase in fecal neutral sterol excretion (Figure 1C) and can be also explained by the LXR-driven reduction in NPC1L1 mRNA levels (Figure S1C) (Duval et al., 2006). As a compensatory physiologic response, hepatic cholesterol synthesis increases in conditions of reduced intestinal cholesterol absorption (Repa et al., 2005). Consistently, in vivo de novo hepatic cholesterol synthesis was significantly increased by 25% in iVP16LXRα mice compared to control iVP16 mice (Figure 1D). Unchanged cholesterol synthesis observed in the kidney (Figure 1D) confirmed the hepatic selective adaptive response. In line with these results, hepatic genes involved in cholesterol biosynthesis, i.e., SREBP2, HMG-CoA synthase, and HMG-CoA reductase, were upregulated in the liver of iVP16LXRα mice Figure S1E. Thus, intestinal selective LXR activation results in reduced intestinal cholesterol absorption and increased hepatic de novo cholesterol synthesis.

To investigate the metabolic effect of selective LXR activation in the intestine, we first analyzed plasma cholesterol levels in lipoproteins. iVP16LXRα displayed an increase in total cholesterol levels (Figure 1E) and HDL cholesterol particles (Figure 1F). Moreover, two-dimensional gel electrophoresis showed a significant increase in the preβ-HDL fraction (Figures 1G and 1H), highlighting the important contribution of the intestine to the synthesis of these particles. To test whether the preβ-HDL formation could lead to increased RCT, we carried out an in vivo study in which ^{3}H-cholesterol-labeled J774 cells were peritoneally injected into iVP16LXRα and control iVP16 mice. As shown in Figure 1I, biliary and fecal ^{3}H-cholesterol levels were increased while ^{3}H-bile acid levels were unchanged, suggesting that in iVP16LXRα mice bile acid synthesis was unaffected, as also confirmed by the unaltered CYP7A1 mRNA levels

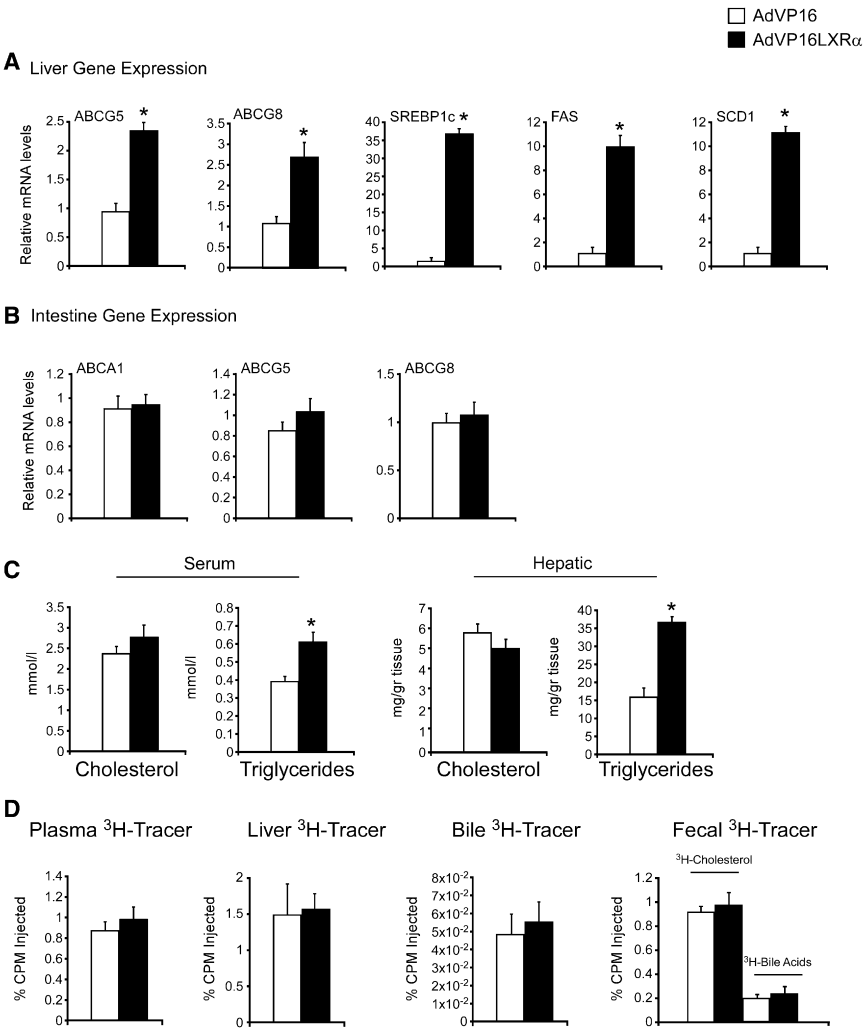

Figure 2. Hepatic-Specific LXR Activation Does Not Affect RCT

(A) Significant upregulation of LXR target genes ABCG5, ABCG8, SREBP1c, FAS, and SCD1 was observed in the liver of mice infected with AdVP16LXRα compared to control AdVP16 infected mice.

(B) Intestinal gene expression levels of LXR targets ABCA1, ABCG5, and ABCG8 did not change after AdVP16 and AdVP16LXRα infection, thus underlining the hepatic-specific LXR activation.

(C) Serum and hepatic cholesterol and TG levels were measured in AdVP16 and AdVP16LXRα infected mice. Data show increased TG levels in both serum and liver with a trend toward a reduction in hepatic cholesterol levels.

(D) Macrophage-derived ^{3}H-cholesterol content in plasma, liver, bile, and feces was measured by liquid scintillation counting. Data analysis shows that hepatic-specific LXR activation did not alter the macrophage-mediated RCT. The results are shown as mean ± SEM (n = 6 for each Ad-infected animal) and are expressed as percent of radioactivity injected. *p < 0.05 AdVP16LXRα versus AdVP16.

and hepatic 7α-hydroxy-4-cholesten-3-one (C4) that was used to monitor CYP7A1 enzymatic activity (Galman et al., 2003) (Figures S1F and S1G). Taken together, these data show that the intestinal activation of LXRα affects plasma lipoproteins, increases preβ-HDL formation, and promotes macrophage-mediated RCT, which results in enhanced fecal cholesterol disposal.

Hepatic LXR Activation Does Not Contribute to RCT

Since the liver is also an important player in regulating cholesterol HDL metabolism, we checked whether activation of hepatic LXR could contribute to RCT in vivo. We generated adenoviruses expressing the same VP16LXRα and VP16 control chimera proteins of the transgenic mice. These viruses were functional in human cell lines (Figures S2A and S2B). We then injected 5 × 10^{9} pfu/ml of AdVP16 or AdVP16LXRα in the jugular vein of 12-week-old male mice on the same pure strain FVBN background of the iVP16 and iVP16LXRα mice. Hepatic-specific LXRα activation induced significant upregulation of all LXR target genes ABCG5, ABCG8, SREBP1c, FAS, and SCD1 in the liver (Figure 2A), but not in the intestine (Figure 2B), of AdVP16LXRα mice. These molecular events were coupled with significant increase in both hepatic and plasma triglycerides (TG) (most probably induced by the increased hepatic de novo lipogenesis via SREBP1c activation) with a trend for the overall decrease in the hepatic cholesterol (Figure 2C) and no significant changes in the circulating pre-βHDL levels (data not shown). The in vivo RCT experiment revealed the absence of changes in the radiolabeled index in the plasma, liver, bile, and fecal cholesterol (Figure 2D). Thus, at a variance of RCT data obtained with systemic LXR ligands (Naik et al., 2006) and intestinal-specific LXRα activation (Figure 1I), hepatic-specific LXRα activation does not promote cholesterol transport in vivo from macrophages to feces.

Reduced Hepatic Cholesterol Esters and TG in iVP16LXRα Mice

To investigate whether iVP16LXRα mice are resistant to high dietary cholesterol, we challenged these mice with a 2% cholesterol-enriched diet (Peet et al., 1998). The cholesterol-enriched diet activated hepatic LXR to similar extent in iVP16LXRα and iVP16 mice, as shown by the induction in ABCG5-ABCG8 mRNA levels (Figure S3A). Similarly, intestinal ABCA1, ABCG5, and ABCG8 mRNA levels were upregulated in iVP16 mice and to a lesser extent also in iVP16LXRα mice, where the basal levels were already induced (Figure S3B). Livers from control mice showed a change in color saturation and appeared whitish, a hallmark of lipid accumulation; on the contrary, the color saturation was unmodified in the livers of iVP16LXRα mice after high-cholesterol diet (Figure 3A). Reduced accumulation of hepatic

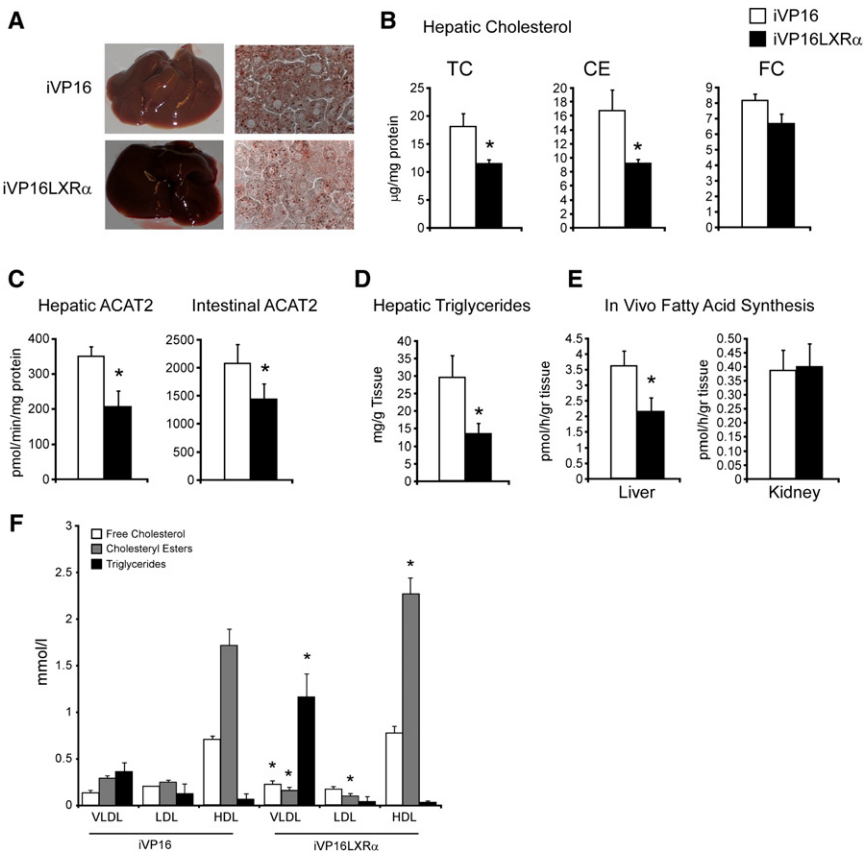

Figure 3. Hepatic and Plasma Cholesterol and TG Content in iVP16LXRα after High-Cholesterol Diet

(A) Macroscopic appearance and oil red O staining of livers from iVP16 and iVP16LXRα mice after 2% cholesterol diet.

(B) Hepatic cholesterol subtypes in iVP16 and iVP16LXRα mice on high-cholesterol diet. iVP16 mice showed a 30% increase of total liver cholesterol (TC) amount after high-cholesterol diet compared to iVP16LXRα mice. This difference was identified as a difference in cholesterol esters (CE). Free cholesterol (FC) was unmodified.

(C) Hepatic and intestinal ACAT2 enzymatic activity. Data analysis shows a significant difference in both hepatic and intestinal ACAT2 activity between iVP16LXRα and control mice after high-cholesterol diet.

(D) Hepatic TG content after 2% cholesterol diet. High-cholesterol diet resulted in a strong increase of hepatic TG levels in iVP16 mice contrarily to iVP16LXRα.

(E) The rates of in vivo fatty acids synthesis in the liver and kidney (extrahepatic control tissue) of transgenic mice after high-cholesterol diet was measured 60 min after intraperitoneal injection of ^{3}H-water precursor. iVP16LXRα showed a reduction in de novo fatty acids after high-cholesterol diet.

(F) Free cholesterol, cholesterol esters, and TG lipoprotein measurements after separation by SEC in iVP16LXRα and iVP16 mice fed a high-cholesterol diet. iVP16LXRα showed a significant increase in HDL cholesterol and VLDL-TG particles compared to control mice, with significant reduction in VLDL-CE content. The results are shown as mean ± SEM (n = 6 for each genotype). *p < 0.05 iVP16LXRα versus VP16.

lipids in iVP16LXRα mice under high-cholesterol diet was confirmed by oil red O analysis (Figure 3A). Hepatic lipid analysis showed 30% higher total cholesterol amount (TC) of iVP16 mice after the 2% cholesterol diet compared to iVP16LXRα (Figure 3B). Also, iVP16LXRα presented significantly lower CE levels in the liver compared with control iVP16 mice, while FC levels did not change (Figure 3B). To verify whether the observed differences in CE amount were related to modifications in the activity of the ACAT2 enzyme, which is a key enzyme involved in the esterification of cholesterol, ACAT2 activity was analyzed both in the liver and in the intestine. iVP16LXRα mice presented a strong reduction in ACAT2 activity, especially in the liver (Figure 3C). A well-known side effect of systemic LXR activation as well as of a high-cholesterol diet is the increase of hepatic TG synthesis. To evaluate whether selective intestinal LXR activation prevented the increase in hepatic TG in a high-cholesterol diet, we determined hepatic TG levels in the transgenic mice after high-cholesterol diet. High-cholesterol diet resulted in elevated hepatic TG in iVP16 control mice. On the contrary, iVP16LXRα mice showed significantly lower hepatic TG accumulation (Figure 3D). Analysis of the in vivo hepatic fatty acid synthesis confirmed the reduction in the de novo fatty acid synthesis rate in iVP16LXRα after high-cholesterol diet compared to control iVP16 mice (Figure 3E). Equal in vivo fatty acid synthesis rate in the kidney of both control iVP16 and iVP16LXRα mice confirmed the hepatic selective response. The analysis of lipoprotein profiles confirmed the increase in HDL cholesterol in iVP16LXRα mice and no differences in cholesterol levels in VLDL and LDL particles (Figure 3F) also during high-cholesterol diet. In contrast, iVP16LXRα mice presented a VLDL fraction proportionally more enriched in TG than that observed in iVP16 mice. The VLDL particles of iVP16LXRα were enriched in TG to replace the CE that were fewer (Figure 3F), thus being not atherosclerotic as in the *ACAT2*$^{-/-}$ mouse model (Willner et al., 2003). Taken together, these data show that intestinal selective LXR activation protects against high-cholesterol-diet-induced hepatic steatosis, in the absence of any increase of fatty acid synthesis.

Antiatherogenic Effects of Intestinal LXR Activation

To investigate whether the observed changes in lipid profile and increase in RCT affected atherosclerosis, we crossed iVP16LXRα and iVP16 mice with the *LDLR*$^{-/-}$ mice. The resulting *iVP16/LDLR*$^{-/-}$ and *iVP16LXRα/LDLR*$^{-/-}$ mice were fed with an atherogenic high-fat Western diet for 16 weeks. Intestinal LXR targets ABCA1, ABCG5, and ABCG8 were significantly upregulated by the diet in both *iVP16/LDLR*$^{-/-}$ and *iVP16LXRα/LDLR*$^{-/-}$ mice (Figure 4A). Quantification of Sudan IV-stained

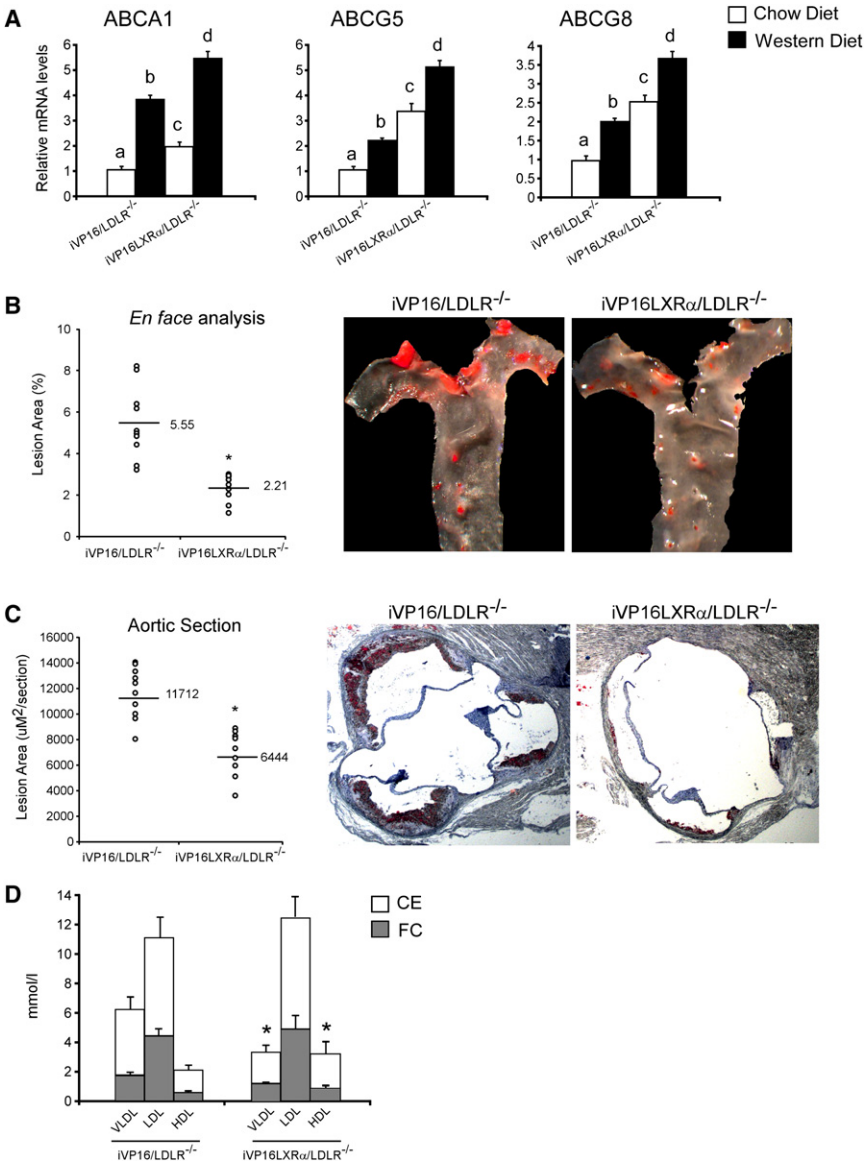

Figure 4. Antiatherogenic Effects of Intestinal LXRα Activation

(A) Expression of ABCA1, ABCG5, and ABCG8, in the intestine of *iVP16LXRα/LDLR*$^{-/-}$ and *iVP16/LDLR*$^{-/-}$ mice under chow and atherogenic Western diet was measured by real-time quantitative PCR. The results are shown as mean ± SEM (n = 6 for each genotype). Different lowercase letters indicate statistical difference ($p < 0.05$).

(B and C) En face and aortic root analysis of atherosclerosis in *iVP16LXRα/LDLR*$^{-/-}$ and *iVP16/LDLR*$^{-/-}$ mice. Atherosclerotic lesions in entire aorta and lesion area of aortic root were quantified as reported in the Supplemental Experimental Procedures. Intestinal-specific activation of LXRα inhibited the development of atherosclerotic lesions in aorta and aortic root.

(D) *iVP16LXRα/LDLR*$^{-/-}$ and *iVP16/LDLR*$^{-/-}$ mice presented similar levels of atherogenic LDL cholesterol lipoproteins, with a similar ratio of FC/CE. Compared to *iVP16/LDLR*$^{-/-}$ mice, *iVP16LXRα/LDLR*$^{-/-}$ presented a significant decrease in the VLDL cholesterol levels with lower CE amounts while showing 15% increase in HDL cholesterol with higher CE levels. *$p < 0.05$ *iVP16LXRα/LDLR*$^{-/-}$ versus *iVP16/LDLR*$^{-/-}$.

en face preparation of the aorta revealed a dramatic reduction in atherosclerotic lesions in *iVP16LXRα/LDLR*$^{-/-}$ mice compared to *iVP16/LDLR*$^{-/-}$mice (Figure 4B). We than analyzed aortic root sections from male *iVP16/LDLR*$^{-/-}$ and *iVP16LXRα/LDLR*$^{-/-}$ mice. Quantification of lesions after oil red O staining disclosed a significant reduction in lesion areas in *iVP16LXRα/LDLR*$^{-/-}$ mice compared with control *iVP16/LDLR*$^{-/-}$ mice (Figure 4C). Interestingly, *iVP16LXRα/LDLR*$^{-/-}$ and *iVP16/LDLR*$^{-/-}$ mice presented similar levels of atherogenic LDL cholesterol lipoproteins, with a similar ratio of FC/CE (Figure 4D). On the other hand, compared to *iVP16/LDLR*$^{-/-}$ mice, *iVP16LXRα/LDLR*$^{-/-}$ presented a significant decrease in the VLDL cholesterol levels with lower CE amounts while showing 15% increase in HDL cholesterol with higher CE levels. Thus, the specific activation of LXR in the intestine protects against atheroclerosis.

DISCUSSION

The present work provides clear evidence of the direct link between intestinal-specific LXR activation and atherosclerosis protection. The specific intestinal expression of the constitutively activated form of LXRα determined the upregulation of intestinal LXR target genes involved in cholesterol secretion on both luminal (ABCG5 and ABCG8) and plasma (ABCA1) compartments. This dual upregulation resulted in a strong reduction of cholesterol absorption as well as in an increase of pre-βHDL particles, which are excellent acceptors of cholesterol secreted by the macrophages as shown by the upregulation in the RCT pathway. In line with our finding, elegant pharmacological studies have previously demonstrated a net induction of the RCT pathway after targeting intestinal LXR (Brunham et al., 2006b; Peng et al., 2008; Yasuda et al., 2010). Nevertheless, since even moderate decrease in the intestinal cholesterol absorption rates are associated with a large atherosclerotic protection (Greenberg et al., 2009), deletion of NPC1L1 or treatments with ezetimibe in the iVP16LXRα mice are needed to finally dissect the importance of the apical versus basolateral enterocyte LXR activation in the protection against atherosclerosis.

In the present study, we also show that hepatic-specific LXR activation via adenoviral infection did not induce any significant changes in the RCT pathway, thus underlining the importance of the intestine in this respect. Furthermore, using the transgenic iVP16LXRα mice, we proved that the metabolic effects of

intestinal-specific LXR activation became more apparent when mice were fed a high-cholesterol diet or in *iVP16LXRα/LDLR*$^{-/-}$ mice fed an atherogenic Western diet. Indeed, iVP16LXRα mice were protected from hepatic cholesterol accumulation. In particular, hepatic CE was decreased as a consequence of reduced hepatic ACAT2 activity. In iVP16LXRα, the lower ACAT2 activity was associated to decreased TG content in the liver (Figures 3C–3E) and to increased plasma VLDL-TG (Figure 3F). Hence, the reduction of total hepatic TG and the unaffected in vivo hepatic fatty acids synthesis were likely due to an increased efflux of TG from the liver in iVP16LXRα mice to replace CE in VLDL (Figure 3F). Finally, en face and aortic root analysis of *iVP16LXRα/LDLR*$^{-/-}$ athero-susceptible mice with no changes in atherogenic LDL cholesterol particles clearly indicated that, together with the reduced intestinal cholesterol absorption, the increased synthesis in HDL and the reduction in ACAT2 activity observed in the intestinal-specific LXR transgenic mice protects from atherosclerosis without any side effects such as liver steatosis and increased fatty acid synthesis.

In conclusion, this work provides the molecular-metabolic scenario to highlight the critical role of intestinal-specific LXR activation for the regulation of cholesterol homeostasis in the body and the potential of this strategy in the treatment of cardiovascular disease.

EXPERIMENTAL PROCEDURES

Animal Generation, Maintenance, and Treatments

The intestinal-specific VP16LXRα transgenic mice (iVP16LXRα) were generated by injecting the pSKVillin-VP16LXRα plasmid digested with HpaI into the pronuclei of the fertilized eggs of FVB/N mice. First, the VP16LXRα (1.5 Kb) fragment with XhoI and SacII restriction sites was generated by PCR from the pCMX-VP16LXRα plasmid (kindly provided by Dr. D.J. Mangelsdorf). Then the fragment was subcloned at the XhoI and SacII restriction sites downstream of the villin promoter region of the pSKVillin plasmid (kindly provided by Dr. D. Gumucio). The specific control mice (iVP16) were generated with the same strategy. The coding sequence of herpes simplex transactivation domain VP16 was subcloned downstream the villin promoter region of the pSKVillin plasmid. Liver, kidney, stomach, jejunum, duodenum, ileum, and colon of transgenic mice were dissected and prepared for total RNA extraction to evaluate the specific intestinal expression of transgene under the villin promoter control. Mice were hosted under standard 12 hr light/12 hr dark cycle and fed standard rodent chow and water ad libitum. Where indicated, this diet was supplemented with 2% (w/w) cholesterol (DP1014 Altromin; RIEPER; Vandoies, BZ) (Peet et al., 1998). *LDLR*$^{-/-}$ mice on a C57BL/6 background were obtained from The Jackson Laboratory. *LDLR*$^{-/-}$ mice were crossed with the iVP16LXRα and control iVP16 mice to obtain at the F2 generation the *iVP16LXRα/LDLR*$^{-/-}$ and the control *iVP16/LDLR*$^{-/-}$ mice in a mixed strain background. These mice were backcrossed for eight generations to obtain the exact number of mice used in our experiment. For atherosclerosis studies, *iVP16LXRα/LDLR*$^{-/-}$ or *iVP16/LDLR*$^{-/-}$ crossed mice were placed on a Western diet (DP1014mod. RIEPER) containing 0.2% cholesterol and 21.2% fat for 16 weeks prior to sacrifice. Ten- or twelve-week-old male mice were used in each group of experiments. The Ethical Committee of the Consorzio Mario Negri Sud approved this experimental setup, which was also certified by the Italian Ministry of Health in accordance with internationally accepted guidelines for animal care.

SUPPLEMENTAL INFORMATION

Supplemental Information includes Supplemental Experimental Procedures, Supplemental References, and three figures and can be found with this article online at doi:10.1016/j.cmet.2010.07.002.

ACKNOWLEDGMENTS

We thank V. Cardile, A.K. Groen, D. Gumucio, D.J. Mangelsdorf, G. Palasciano, G. Tognoni, and G. Villani for tools and discussion; Telethon Core Facility for Conditional Mutagenesis at the Istituto Scientifico San Raffaele (Milano) for generating transgenic mice; R. Ledonne, G. Di Tullio, A. D'Orazio, and C. Di Filippo for technical assistance. This work was funded by Italian Ministry of Health and Education (Finanziamenti per la Ricerca di Base -IDEAS-RBID08C9N7), Italian Association for Cancer Research (AIRC, Milan, Italy), European Community's Seventh Framework Programme FP7/2007– 013 under Grant Agreement No. 202272 (LipidomicNet), Telethon Foundation (GPP08259), Cariplo Foundation Milan, University of Bari, Italy. S.M. is a fellow of CariSPAQ (L'Aquila, Italy). G.L.S. is a fellow of AIRC (Milan, Italy).

Received: October 28, 2009
Revised: April 11, 2010
Accepted: June 7, 2010
Published: August 3, 2010

REFERENCES

Brunham, L.R., Kruit, J.K., Iqbal, J., Fievet, C., Timmins, J.M., Pape, T.D., Coburn, B.A., Bissada, N., Staels, B., Groen, A.K., et al. (2006a). Intestinal ABCA1 directly contributes to HDL biogenesis in vivo. J. Clin. Invest. *116*, 1052–1062.

Brunham, L.R., Kruit, J.K., Pape, T.D., Parks, J.S., Kuipers, F., and Hayden, M.R. (2006b). Tissue-specific induction of intestinal ABCA1 expression with a liver X receptor agonist raises plasma HDL cholesterol levels. Circ. Res. *99*, 672–674.

Duval, C., Touche, V., Tailleux, A., Fruchart, J.C., Fievet, C., Clavey, V., Staels, B., and Lestavel, S. (2006). Niemann-Pick C1 like 1 gene expression is down-regulated by LXR activators in the intestine. Biochem. Biophys. Res. Commun. *340*, 1259–1263.

Galman, C., Arvidsson, I., Angelin, B., and Rudling, M. (2003). Monitoring hepatic cholesterol 7alpha-hydroxylase activity by assay of the stable bile acid intermediate 7alpha-hydroxy-4-cholesten-3-one in peripheral blood. J. Lipid Res. *44*, 859–866.

Greenberg, M.E., Smith, J.D., and Sehayek, E. (2009). Moderately decreased cholesterol absorption rates are associated with a large atheroprotective effect. Arterioscler. Thromb. Vasc. Biol. *29*, 1745–1750.

Grefhorst, A., Elzinga, B.M., Voshol, P.J., Plosch, T., Kok, T., Bloks, V.W., van der Sluijs, F.H., Havekes, L.M., Romijn, J.A., Verkade, H.J., and Kuipers, F. (2002). Stimulation of lipogenesis by pharmacological activation of the liver X receptor leads to production of large, triglyceride-rich very low density lipoprotein particles. J. Biol. Chem. *277*, 34182–34190.

Janowski, B.A., Willy, P.J., Devi, T.R., Falck, J.R., and Mangelsdorf, D.J. (1996). An oxysterol signalling pathway mediated by the nuclear receptor LXR alpha. Nature *383*, 728–731.

Joseph, S.B., McKilligin, E., Pei, L., Watson, M.A., Collins, A.R., Laffitte, B.A., Chen, M., Noh, G., Goodman, J., Hagger, G.N., et al. (2002). Synthetic LXR ligand inhibits the development of atherosclerosis in mice. Proc. Natl. Acad. Sci. USA *99*, 7604–7609.

Klucken, J., Buchler, C., Orso, E., Kaminski, W.E., Porsch-Ozcurumez, M., Liebisch, G., Kapinsky, M., Diederich, W., Drobnik, W., Dean, M., et al. (2000). ABCG1 (ABC8), the human homolog of the Drosophila white gene, is a regulator of macrophage cholesterol and phospholipid transport. Proc. Natl. Acad. Sci. USA *97*, 817–822.

Kratzer, A., Buchebner, M., Pfeifer, T., Becker, T.M., Uray, G., Miyazaki, M., Miyazaki-Anzai, S., Ebner, B., Chandak, P.G., Kadam, R.S., et al. (2009). Synthetic LXR agonist attenuates plaque formation in apoE−/− mice without inducing liver steatosis and hypertriglyceridemia. J. Lipid Res. *50*, 312–326.

Laffitte, B.A., Repa, J.J., Joseph, S.B., Wilpitz, D.C., Kast, H.R., Mangelsdorf, D.J., and Tontonoz, P. (2001). LXRs control lipid-inducible expression of the apolipoprotein E gene in macrophages and adipocytes. Proc. Natl. Acad. Sci. USA *98*, 507–512.

Linsel-Nitschke, P., and Tall, A.R. (2005). HDL as a target in the treatment of atherosclerotic cardiovascular disease. Nat. Rev. Drug Discov. *4*, 193–205.

Madison, B.B., Dunbar, L., Qiao, X.T., Braunstein, K., Braunstein, E., and Gumucio, D.L. (2002). Cis elements of the villin gene control expression in restricted domains of the vertical (crypt) and horizontal (duodenum, cecum) axes of the intestine. J. Biol. Chem. *277*, 33275–33283.

Naik, S.U., Wang, X., Da Silva, J.S., Jaye, M., Macphee, C.H., Reilly, M.P., Billheimer, J.T., Rothblat, G.H., and Rader, D.J. (2006). Pharmacological activation of liver X receptors promotes reverse cholesterol transport in vivo. Circulation *113*, 90–97.

Navab, M., Hama, S.Y., Anantharamaiah, G.M., Hassan, K., Hough, G.P., Watson, A.D., Reddy, S.T., Sevanian, A., Fonarow, G.C., and Fogelman, A.M. (2000). Normal high density lipoprotein inhibits three steps in the formation of mildly oxidized low density lipoprotein: steps 2 and 3. J. Lipid Res. *41*, 1495–1508.

Oram, J.F., and Vaughan, A.M. (2000). ABCA1-mediated transport of cellular cholesterol and phospholipids to HDL apolipoproteins. Curr. Opin. Lipidol. *11*, 253–260.

Peet, D.J., Turley, S.D., Ma, W., Janowski, B.A., Lobaccaro, J.M., Hammer, R.E., and Mangelsdorf, D.J. (1998). Cholesterol and bile acid metabolism are impaired in mice lacking the nuclear oxysterol receptor LXR alpha. Cell *93*, 693–704.

Peng, D., Hiipakka, R.A., Dai, Q., Guo, J., Reardon, C.A., Getz, G.S., and Liao, S. (2008). Antiatherosclerotic effects of a novel synthetic tissue-selective steroidal liver X receptor agonist in low-density lipoprotein receptor-deficient mice. J. Pharmacol. Exp. Ther. *327*, 332–342.

Rader, D.J. (2002). High-density lipoproteins and atherosclerosis. Am. J. Cardiol. *90*, 62i–70i.

Rader, D.J. (2003). Regulation of reverse cholesterol transport and clinical implications. Am. J. Cardiol. *92*, 42J–49J.

Repa, J.J., Liang, G., Ou, J., Bashmakov, Y., Lobaccaro, J.M., Shimomura, I., Shan, B., Brown, M.S., Goldstein, J.L., and Mangelsdorf, D.J. (2000a). Regulation of mouse sterol regulatory element-binding protein-1c gene (SREBP-1c) by oxysterol receptors, LXRalpha and LXRbeta. Genes Dev. *14*, 2819–2830.

Repa, J.J., Turley, S.D., Lobaccaro, J.A., Medina, J., Li, L., Lustig, K., Shan, B., Heyman, R.A., Dietschy, J.M., and Mangelsdorf, D.J. (2000b). Regulation of absorption and ABC1-mediated efflux of cholesterol by RXR heterodimers. Science *289*, 1524–1529.

Repa, J.J., Berge, K.E., Pomajzl, C., Richardson, J.A., Hobbs, H., and Mangelsdorf, D.J. (2002). Regulation of ATP-binding cassette sterol transporters ABCG5 and ABCG8 by the liver X receptors alpha and beta. J. Biol. Chem. *277*, 18793–18800.

Repa, J.J., Turley, S.D., Quan, G., and Dietschy, J.M. (2005). Delineation of molecular changes in intrahepatic cholesterol metabolism resulting from diminished cholesterol absorption. J. Lipid Res. *46*, 779–789.

Schultz, J.R., Tu, H., Luk, A., Repa, J.J., Medina, J.C., Li, L., Schwendner, S., Wang, S., Thoolen, M., Mangelsdorf, D.J., et al. (2000). Role of LXRs in control of lipogenesis. Genes Dev. *14*, 2831–2838.

Terasaka, N., Hiroshima, A., Koieyama, T., Ubukata, N., Morikawa, Y., Nakai, D., and Inaba, T. (2003). T-0901317, a synthetic liver X receptor ligand, inhibits development of atherosclerosis in LDL receptor-deficient mice. FEBS Lett. *536*, 6–11.

van der Velde, A.I., Vrins, C.L., van den Oever, K., Kunne, C., Oude Elferink, R.P., Kuipers, F., and Groen, A.K. (2007). Direct intestinal cholesterol secretion contributes significantly to total fecal neutral sterol excretion in mice. Gastroenterology *133*, 967–975.

Venkateswaran, A., Laffitte, B.A., Joseph, S.B., Mak, P.A., Wilpitz, D.C., Edwards, P.A., and Tontonoz, P. (2000). Control of cellular cholesterol efflux by the nuclear oxysterol receptor LXR alpha. Proc. Natl. Acad. Sci. USA *97*, 12097–12102.

Wang, N., Lan, D., Chen, W., Matsuura, F., and Tall, A.R. (2004). ATP-binding cassette transporters G1 and G4 mediate cellular cholesterol efflux to high-density lipoproteins. Proc. Natl. Acad. Sci. USA *101*, 9774–9779.

Willner, E.L., Tow, B., Buhman, K.K., Wilson, M., Sanan, D.A., Rudel, L.L., and Farese, R.V., Jr. (2003). Deficiency of acyl CoA:cholesterol acyltransferase 2 prevents atherosclerosis in apolipoprotein E-deficient mice. Proc. Natl. Acad. Sci. USA *100*, 1262–1267.

Willy, P.J., and Mangelsdorf, D.J. (1997). Unique requirements for retinoid-dependent transcriptional activation by the orphan receptor LXR. Genes Dev. *11*, 289–298.

Yasuda, T., Grillot, D., Billheimer, J.T., Briand, F., Delerive, P., Huet, S., and Rader, D.J. (2010). Tissue-specific liver x receptor activation promotes macrophage reverse cholesterol transport in vivo. Arterioscler. Thromb. Vasc. Biol. *30*, 781–786.

Zilversmit, D.B. (1979). Atherogenesis: a postprandial phenomenon. Circulation *60*, 473–485.